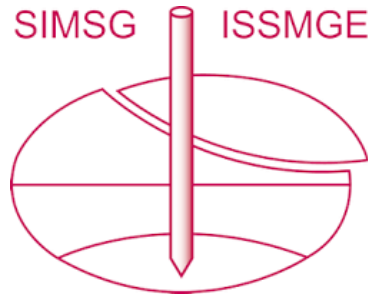


# INTERNATIONAL SOCIETY FOR SOIL MECHANICS AND GEOTECHNICAL ENGINEERING



*This paper was downloaded from the Online Library of the International Society for Soil Mechanics and Geotechnical Engineering (ISSMGE). The library is available here:*

<https://www.issmge.org/publications/online-library>

*This is an open-access database that archives thousands of papers published under the Auspices of the ISSMGE and maintained by the Innovation and Development Committee of ISSMGE.*

*The paper was published in the proceedings of the 10th European Conference on Numerical Methods in Geotechnical Engineering and was edited by Lidija Zdravkovic, Stavroula Kontoe, Aikaterini Tsiampousi and David Taborda. The conference was held from June 26<sup>th</sup> to June 28<sup>th</sup> 2023 at the Imperial College London, United Kingdom.*

*To see the complete list of papers in the proceedings visit the link below:*

<https://issmge.org/files/NUMGE2023-Preface.pdf>

# Parametric finite element analysis of an unsaturated tailings dry stack

J. Barbaran<sup>1</sup>, L. Zdravkovic<sup>1</sup>, D. Potts<sup>1</sup>, J. Quinn<sup>2</sup>

<sup>1</sup>*Department of Civil and Environmental Engineering, Imperial College London, London, UK*

<sup>2</sup>*Klohn Crippen Berger Ltd, York, UK*

**ABSTRACT:** Dry stacks are filtered tailings facilities increasingly used in the mining industry due to their advantages over conventional tailings facilities. One of the main benefits dry stacks offer is an improvement in the facility's physical stability given its unsaturated condition, contrary to conventional tailings, which are primarily slurry-deposited and need large dams to be contained. After the milling process, tailings particle size ranges from fine sands to clays, exhibiting a wide range of unsaturated soil properties. This work studies a dry stack behaviour through a parametric finite element analysis, where the performance of three copper-derived tailings is compared. The analysed tailings correspond to a silty sand (SM), a low plasticity clayey silt (ML-CL) and a low plasticity clay (CL) and are characterised by different soil water retention curves (SWRC). The study shows that capillarity plays a key role in water table elevations for low permeability soils, and that the effect of suction contributes to compressibility reductions and apparent cohesion increases after consolidation of such facilities.

**Keywords:** Filtered tailings; dry stack; unsaturated soils; finite element analysis.

## 1 INTRODUCTION

The mining industry has a key role in providing minerals and metals vital for most aspects of modern life. The production of tailings is inherent to the mining activity and it has increased at a fast pace over the years. The traditional slurry deposition scenario of tailings has brought an increasing number of dam failures around the globe, which imposes the need for investigating and adopting new tailings management strategies.

Filtered tailings are a relatively new management strategy, where tailings are dewatered to a solid content greater than 85%, achieving the consistency of a compactable material (Cooke, 2010). This type of tailings is piled forming a "dry stack" with no need for a large dam to contain it. The benefits of filtered tailings are many, including a reduction of the facility footprint, improvement in the facility's physical stability and enabling progressive closure and reclamation (Engels, 2021).

From a soil mechanics perspective, filtered tailings are unsaturated materials, which makes their behaviour complex to predict during construction and ongoing management. This study aims to assess the dry stack behaviour with a parametric finite element (FE) study, employing the finite element code ICFEP (Potts and Zdravkovic, 1999). Three copper-derived tailings are analysed - a silty sand (SM), a low plasticity clayey silt (ML-CL) and a low plasticity clay (CL), differing principally in their water retention characteristics (SWRC).

## 2 STUDY CASE

The study case for this work is a filtered tailings dry stack. The dry stack foundation is composed of a top 6.5 m thick clay layer overlaying a 10 m thick sandy clay layer on a bedrock of a sedimentary clayey rock, to be consistent with the geological scenario required for this tailings technology. A starter dam (Figure 5) is placed downstream to provide initial lateral containment to the dry stack. It is built from a rockfill material with a lateral extent of 54 m at the base and a height of 8 m, with a 2:1 and 3:1 (horizontal to vertical) downstream and upstream slope, respectively.

The dry stack geometry was based on the description of Erickson et al. (2017) for a dry stack project. It reaches a 40 m height with a 3:1 downstream slope and a maximum base width of 380 m in the transversal cross-section (Figure 5). The tailings are assumed to be spread and compacted in layers of 1m, with eight stages of 5 m each, until reaching 40 m height. The time for construction is assumed to be 25 years and a consolidation period after each constructed layer is allowed.

The SM material was based on a study on mine tailing's properties by Qiu and Segoo (2001) and the ML-CL and CL materials were based on a study on water retention curves for mine tailings by Musso and Suazo (2019). Table 1 summarizes the tailings basic properties and Figure 1 presents the SWRCs obtained with the axis translation technique using a pressure plate apparatus.

Table 1 Tailings properties for SM, CL, ML-CL

USCS Classification	SM	ML-CL	CL
Tailings type	Copper	Copper	Copper
Liquid Limit LL (%)	-	19.6	25.2
Plasticity Index PI (%)	-	6.9	10.56
Shrinkage Limit SL (%)	24.4	-	-
Water content $w_i$ (%)	30.1	25.1	37.9
Fines content (%)	18.5	69.3	96.8
Coef. uniformity $C_u$	9.43	0.250	0.038

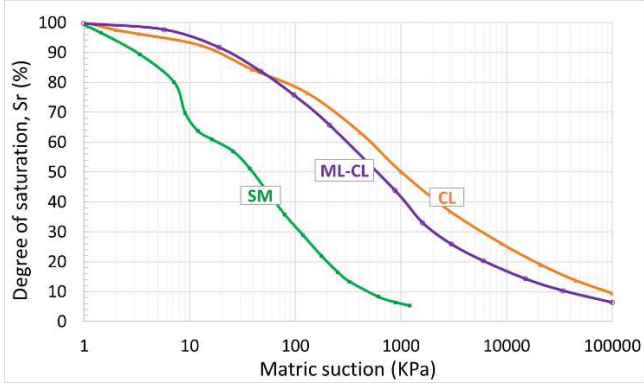


Figure 1. Tailings soil water retention curves (SWRCs)

### 3 METHODOLOGY

#### 3.1 Mechanical model

The tailings mechanical behaviour is modelled using the Imperial College Single Structure Model (ICSSM, Georgiadis et al., 2005), which combines the extended Lagioia et al. (1996) yield surface on the wet side of the critical state and the nonlinear Hvorslev surface (Tsiampousi et al., 2013) on the dry side, see Figure 2.

The model is defined in terms of an equivalent metric suction,  $s_{eq} = s - s_{air}$ , where  $s_{air}$  is an air-entry value of suction. The increase in shear strength due to suction, defined as  $f(s_{eq}) = S_r \cdot s_{eq}$ , is linked to the nonlinear change in the degree of saturation,  $S_r$ .

#### 3.2 SWR model

The soil water retention model used in this study is a Van Genuchten (1980) type model, extended to account for the retention curve dependency on the specific volume. Model parameters in Figure 3 represent the suction at shrinkage limit,  $s_{sl}$ , the suction in the long-term,  $s_o$ , and the degree of saturation in the long-term,  $S_{r0}$ .

#### 3.3 Permeability model

The coefficient of permeability,  $k$ , of an unsaturated soil can be orders of magnitude smaller than that at full saturation. It depends on the volumetric water content and hence on the current value of suction (Fredlund et al.,

1994). A reduction in water content implies lower connectivity of water flow in the pores (Emerman, 2022).

In this study, a suction-dependent permeability model of Nyambayo and Potts (2010), see Figure 4, was adopted. The logarithm of saturated permeability coefficient,  $k_{sat}$ , reduces between the prescribed values of equivalent suction,  $s_1$  and  $s_2$ , until reaching a prescribed minimum value of permeability coefficient,  $k_{min}$ .

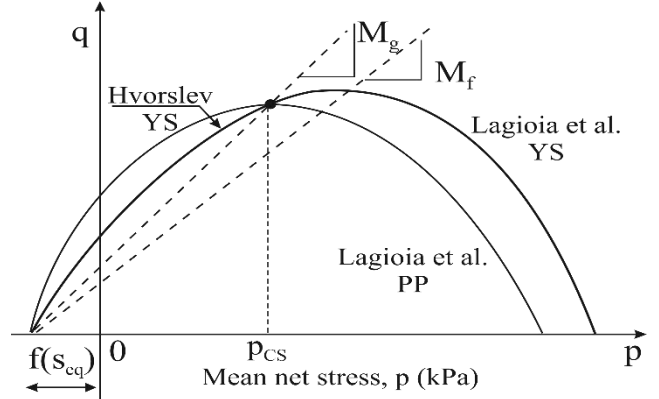


Figure 2. Yield and Plastic Potential functions of the ICSSM

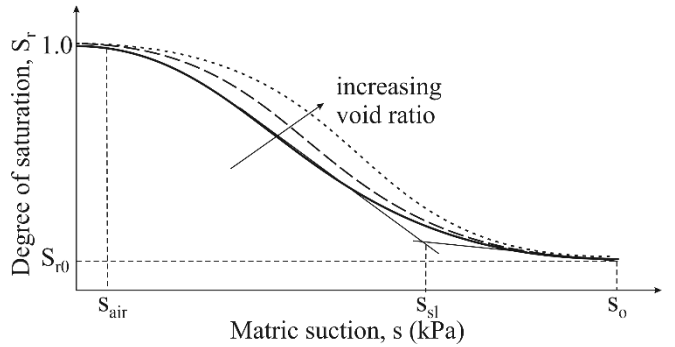


Figure 3. Soil water retention model

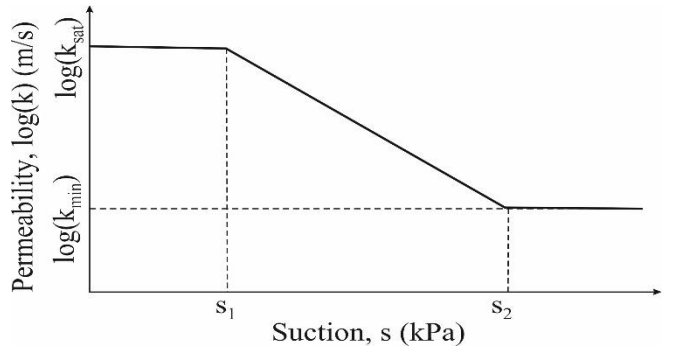


Figure 4. Permeability model

#### 3.4 Material parameters

The calibrated ICSSM parameters are summarised in Table 1, assuming an associated flow rule. The SWR model parameters for the three analysed materials are summarised in Table 2.

The variable permeability is based on a tailings saturated permeability,  $k_{sat} = 10^{-7}$  m/s, for suctions smaller than  $s_1 = s_{air}$  values for each material, and is allowed to decrease to  $k_{min} = 10^{-9}$  m/s at the limit of  $s_2 = 1000$  kPa.

The remaining soils in the analysed domain are represented with a linear elastic Mohr-Coulomb model, with properties summarised in Table 4. The bedrock and the rockfill of the starter dam are treated as drained, while the coefficients,  $k$ , of saturated permeabilities of the top clay and sandy clay layers are assumed constant and equal to  $10^{-8}$  m/s and  $10^{-7}$  m/s, respectively. The thin drainage layer (0.5 m) across the tailings and starter dam bases is assumed highly permeable, with  $k = 10^{-3}$  m/s, to represent a functional drainage.

Table 1. ICSSM parameters

Parameter	Value	Description
$\alpha_g, \alpha_f$	0.4	Plastic potential and Yield surface parameters
$\mu_g, \mu_f$	0.9	
$M_g, M_f$	1.37	Slope of the critical state line in the q-p space in triaxial compression
$p^c$ or $\alpha_c$	1	Characteristic pressure
$\lambda(0)$	0.065	Coefficient of compressibility for saturated condition
$\kappa$	0.008125	Elastic compressibility coefficient
$r$	0.06	Maximum soil stiffness parameter
$\beta$	0.001	Soil stiffness increase parameter
$\kappa_s$	0.001	Elastic compressibility coefficient for changes in suction
$\chi$	0	Factor for the coefficient $\kappa_s$
$\omega$	0	$\kappa_s = (\kappa_{sat})^\chi \cdot (S_r)^\omega$
$v_1$	1.6	Specific volume at unit pressure
OCR	1.1	Overconsolidation ratio
$\mu$	0.3	Poisson ratio
$S_{air}$	1	Air-entry value of suction (kPa)
$K_{min}$	1000	Minimum elastic bulk modulus (kPa)
$S_{oi}$	1000000	Initial hardening parameter for secondary yield surface (suction increase yield curve) (kPa)
$\lambda_s$	0.006	Compressibility coefficient for changes in suction

Table 2. SWR model parameters for SM; CL and ML-CL

Parameter	SM	ML-CL	CL	Description
$S_{air}$	1	1	1	Suction at air-entry value (kPa)
$S_o$	1200	100000	98000	Suction in the long term (kPa)
$S_{ro}$	0.053	0.064	0.095	Degree of saturation in long term
$\alpha$	0.055	0.02	0.028	Fitting parameter
$n$	0.85	0.65	0.57	Fitting parameter
$m$	0.99	0.99	0.9	Fitting parameter
$S_{st}$	325	4000	4000	Suction at shrinkage limit (kPa)

Table 4. Mohr-Coulomb parameters

Material	$E$ (kPa)	$c'$ (kPa)	$\phi'$ (deg)	$\psi$ (deg)
Bedrock	3.8E6	8800	20	0
Sandy clay	1.0E5	1	24	12
Clay	0.5E5	144	22	11
Rockfill	0.5E5	0	40	20

$E$  – Young’s modulus;  $c'$  - cohesion;  $\phi'$  - angle of shearing resistance;  $\psi$  – angle of dilation

### 3.5 Dry stack FE mesh

The dry stack in this study is simulated under plane strain conditions, utilising the assumed symmetry of the problem (Figure 5). The FE mesh comprises 8-noded quadrilateral elements with two displacement degrees of freedom at each node and a pore pressure degree of freedom at corner nodes (only for elements representing consolidating materials).

The initial stresses in the foundation soil are defined by the ground water table at 0.5 m below the ground surface and a hydrostatic pore water pressure profile. The vertical total stresses are defined by the saturated bulk unit weight of 18.9, 20.0 and 20.4 kN/m<sup>3</sup> for the clay, sandy clay, and bedrock, respectively. An earth pressure coefficient at rest,  $K_0 = 1$ , is assumed.

The tailings part of the FE mesh is 40 m in height and is refined to 1m thick element layers to capture the construction sequence and to increase numerical precision. At the beginning of the analysis, when the stresses in the foundation soil are initialised, the starter dam and tailings elements are deactivated from the mesh.

## 4 RESULTS AND DISCUSSION

### 4.1 Phreatic surface in tailings

The simulated deposition of the filtered tailings involves construction, from the ground surface, of consecutive layers of elements, each over a 3.5-month period, by applying their self-weight and compaction properties. The latter assume the suction in a compacted tailings of 30 kPa, void ratio of 0.6 (Erickson et al., 2017) and  $K_0 = 1$ . The value of suction upon compaction results in  $S_r = 55\%$  from the SM retention curve, derived as a minimum average  $S_r$  in a dry stack (Klassen and Quinn, 2021). Each constructed layer is followed by a 3.5-month consolidation period. At the end of tailings construction, a 30 kPa suction boundary condition is applied over the slope and crest of the tailings dam into the long-term.

The coupled nature of the analysis causes gradual redistribution and equilibration of pore pressures within the tailings. The capillary effects lead to the rise of the phreatic surface into the tailings body, shown as an

example for the SM analysis in Figure 6 (a close-up of the tailings only). The interface between the blue and the green shading indicates the position of the phreatic surface (a zero pore water pressure contour), which is the highest at the axis of symmetry, gradually reducing towards the starter dam in which the pore water pressure is set to zero.

The maximum elevation of the phreatic surface for the three tailings types, measured from the base of the stack at the end of their construction, is between 12.2 m

(SM tailings) and 14.5 m (CL tailings), depending on the respective SWR curves. The highest suction of 42.5 kPa is mobilised in the SM tailings and marginally lower in CL and ML-CL tailings (38.5 kPa).

If the permeability of the thin drainage layer is reduced to  $10^{-4}$  m/s, simulating an obstruction in its operation, the phreatic surface rises dramatically to a maximum of 33.3 m, from the tailings base, at the axis of symmetry.

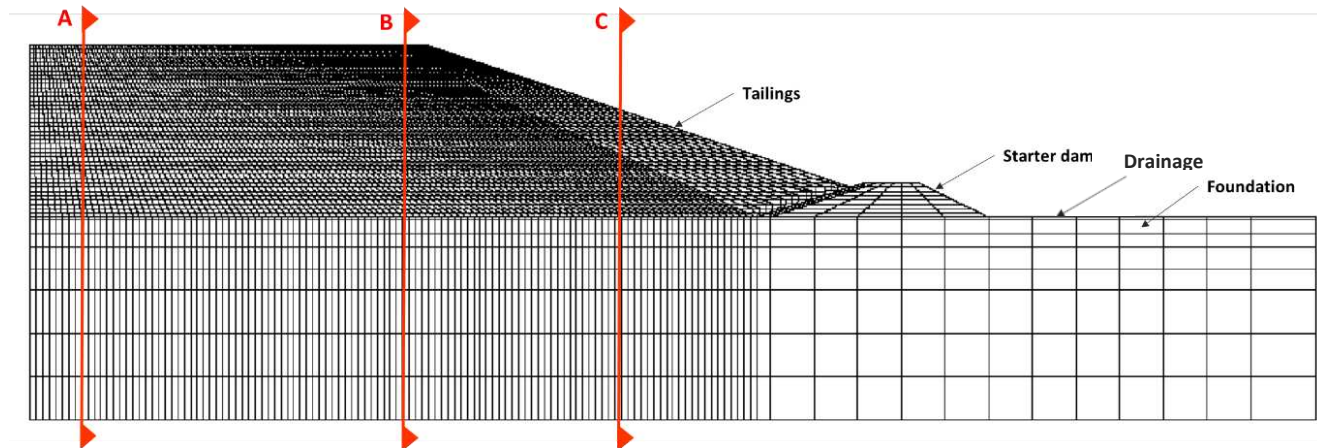


Figure 5. Dry stack finite element mesh, vertical sections for interpretation of analyses results

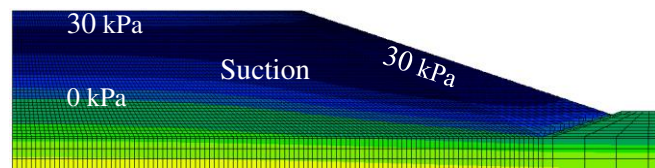


Figure 6. Pore pressure contours at the end of SM tailings construction

As would be expected, the settlements of each tailings are the largest in the central Section A, reducing gradually towards the toe of the dry stack. The effect of the water retention characteristics is marginal but still noticeable in each section, with the SM tailings settling slightly less compared to the two variants which mobilise practically identical magnitudes.

## 4.2 Vertical displacements comparison

### 4.2.1 Dry stack settlements

The coefficient of uniformity,  $C_u$ , and the fines content summarised in Table 1 indicate that the SM tailings should be less compressible than ML-CL and CL variants. However, for the parametric analyses performed here, the mechanical properties in the ICSSM model were maintained the same for all three materials, the objective being to examine the effect of different water retention characteristics, shown in Figure 1 and Table 3.

The tailings settlements are assessed at the three vertical cross-sections indicated in Figure 5, with example profiles shown in Figure 7 for Section C and with maximum settlements summarised in Table 5.

Table 5. Maximum settlements in section A, B and C

Tailings	SM	ML-CL	CL
Section A	1619 mm	1621 mm	1621 mm
Section B	1579 mm	1596 mm	1594 mm
Section C	1121 mm	1137 mm	1136 mm

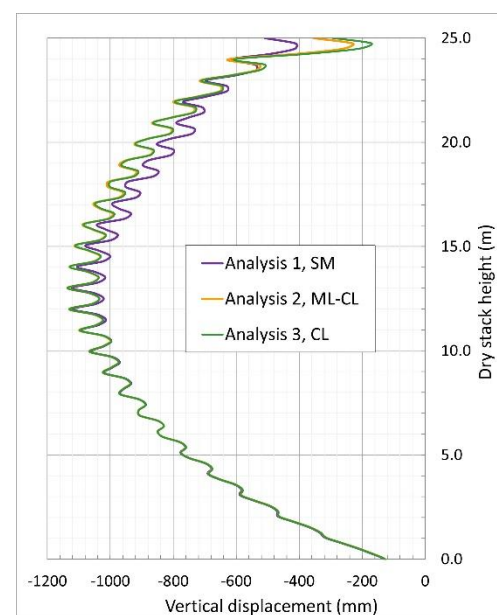


Figure 7. Example settlement profile, Section C

### 4.2.2 Ground settlements

The maximum settlements in the foundation soil, in the range of 183 mm to 188 mm, are predicted in the

centreline of the dry stack, as expected. These values are marginal given the size of the structure above and are a consequence of the ground properties summarised in Table 4 and derived from a dry stack characterisation by Erickson et al. (2017). The slightly different ground settlements caused by each tailings are a consequence of the slightly different elevations of the phreatic surface in each tailings' dry stack, as commented in Section 4.1, given that the density of each of the three tailings materials was maintained the same, at  $2.45 \text{ g/cm}^3$ .

### 4.3 Horizontal displacements comparison

The maximum horizontal displacements at sections A to C in each dry stack are summarised in Table 6. The values are extremely marginal in the central Section A due to the predominantly vertical load transfer in this section. As shear stresses gradually increase towards the dry stack slope, higher lateral movements are mobilised, the largest predicted in Section C.

Table 6. Maximum horizontal displacements

Tailings	SM	ML-CL	CL
Section A	1.7 mm	1.6 mm	1.4 mm
Section B	65 mm	74 mm	73 mm
Section C	172 mm	298 mm	314 mm

In contrast to the tailings settlements discussed above, the differences in the predicted horizontal movements with respect to the tailings type become significantly more pronounced. The finer tailings (ML-CL and CL) are predicted to mobilised on average 70% larger horizontal movements in Section C compared to SM tailings, indicating in Figure 8 an onset of a slip surface at around 2 m depth from the slope surface in this cross-section.

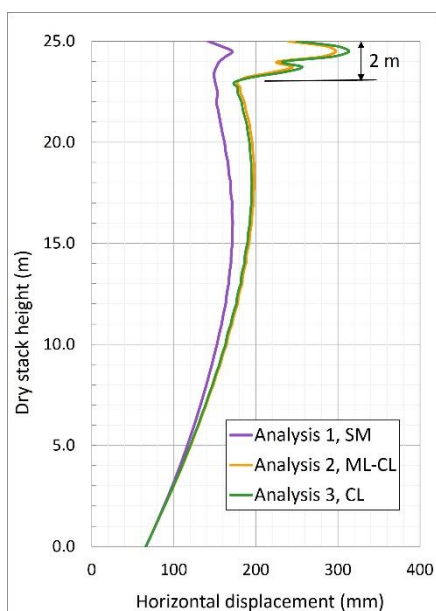


Figure 8. Example lateral movements profile, Section C

### 4.4 Factors of safety comparison

The stability of the three dry stacks was assessed by evaluating a global factor of safety in the tailings slope at the end of construction, before any significant dissipation of pore water pressures may evolve in the long-term. The methodology of the strength reduction in the soil developed in ICFEP is generalised for any soil constitutive model (Potts and Zdravkovic, 2012), including unsaturated models (Zdravkovic et al., 2014). In this approach, the factor of safety on soil strength, known also as a material factor,  $F_m$ , is introduced as an additional state parameter in a constitutive model. Starting from  $F_m = 1$ , the numerical process involves an incremental increase in  $F_m$ , until failure is observed in the FE analysis. The material factor increase imposes an incremental stress reduction from the stress state when  $F_m = 1$ , hence reducing the soil strength according to the following expressions:

$$\phi'_d = \text{atan} \left( \frac{\tan \phi'_{ch}}{F_m} \right)$$

In the above  $\phi'_{ch}$  represents the best estimate value of the angle of shearing resistance from ground investigation, while  $\phi'_d$  is the reduced design value. Additionally, this methodology also affects the right-hand side of the governing FE equations.

This strength reduction process is applied here to the tailings material only and Table 7.7 shows a summary of the predicted factors of safety for the three types of tailings, observing their similarity at  $F_m = 1.3$  on average.

Table 7. Factors of safety

Tailings	SM	ML-CL	CL
Overall material factor $F_m$	1.33	1.28	1.28

It is noted that the analysis increment at which *failure* of a dry stack is established in this study, is determined from a combination of two conditions: the failure of an analysis increment to properly converge and a substantial increase in the magnitude of the horizontal displacements at the crest and mid-side of the tailings slope.

## 5 CONCLUSIONS

The effect of the water retention behaviour in copper-derived tailings materials, on the response of a 40 m high filtered tailings dry stack during its construction, was studied through numerical analyses incorporating advanced modelling capabilities of the finite element software ICFEP. A parametric study was carried out considering three water retention curves, corresponding to a silty sand (SM), a low plasticity clayey silt (ML-

CL) and a low plasticity clay (CL) tailings. The numerical model and material parameters are based on a case study of a dry stack project and on a number of mine tailings studies found in literature. It should be noted that available experimental studies offered very marginal characterisation of these materials in their unsaturated state.

The differences in the water retention behaviour of the examined tailings did not indicate significantly different predicted responses of the dry stack in terms of the mobilised suction magnitudes and phreatic surface locations, settlements, and factors of safety for the dry stack slope. The principal difference was observed in the predicted horizontal movements, where dry stacks with high fines content indicated an onset of a failure surface at 2 m depth in the mid-slope section.

## 6 ACKNOWLEDGEMENTS

The authors acknowledge the financial support of the UK government's Chevening scholarship, programme funded by the Foreign, Commonwealth and Development Office, for the post-graduate MSc programme of J. Barbaran, during which this work was developed.

## 7 REFERENCES

- Cooke, R. 2010. MWH Short Course: Improved Water Recovery through Implementation of Alternative Tailing Disposal Methods. Proceedings 2010 Tailings and Mine Waste Conference. Vail, Colorado.
- Emerman, S. H. 2022. Prediction of Seepage from the Clay Tailings Filter Stack (CTFS) at the Lithium Nevada Thacker Pass Mine, Northern Nevada. Utah, USA, Malach Consulting, LLC.
- Engels, J. 2021. Dry Stacking of Tailings (Filtered Tailings). <https://www.tailings.info/disposal/drystack.htm> [Accessed 01/08/2022].
- Erickson, B., Butikofer, D., Marsh, A., Friedel, R., Murray, L., Piggott, M. 2017. Filtered Tailings Disposal Case History: Operation and Design Considerations Part II. Proceedings International Conference on Tailings and Mine Waste. November 5-8, 2017, Banff, Alberta. Canada, Edmonton, AB: University of Alberta Geotechnical Centre, 2017.7. pp.1-11.
- Fredlund, D. G., Xing, A., Huang, S. 1994. Predicting the permeability function for unsaturated soils using the soil-water characteristic curve. *Canadian Geotechnical Journal*. 31 (4), 533-546.
- Georgiadis, K., Potts D.M., Zdravkovic L. 2005. Development, implementation and application of partially saturated soil models in finite element analysis. Three-dimensional constitutive model for partially and fully saturated soils. *International Journal of Geomechanics*, 5(3), 244-255..
- Klassen, D., Quinn, J. (2021) Geotechnical characterization of a filtered tailings stack. 2021 Tailings and Mine Waste. Proceedings of the 25th international conference on tailings and mine waste. 06 November 2021, University of Alberta. Alberta, Canada.
- Lagioia, R., Puzrin, A. M., Potts, D. M. 1996. A new versatile expression for yield and plastic potential surfaces. *Computers and Geotechnics*. 19 (3), 171-191. 10.1016/0266-352X(96)00005-5.
- Musso, J., Suazo, G. 2019. Determinación de la curva de retención de agua para relaves multimetálicos de la industria minera de Chile. *Obras Y Proyectos*. (25), 22-29. 10.4067/S0718-28132019000100022.
- Nyambayo, V.P., Potts, D.M. 2010. Numerical simulation of evapotranspiration using a root water uptake model. 2010. *Computers and Geotechnics* 37: 175-186.
- Potts, D.M., Zdravkovic, I. 1999. *Finite element analysis in geotechnical engineering; theory*. Thomas Telford Publishing, London, UK.
- Potts, D.M., Zdravkovic, L. 2012. Accounting for partial material factors in numerical analysis. *Géotechnique* 62 (12): 1053-1065.
- Qiu, Y., Sego, D. C. 2001. Laboratory Properties of Mine Tailings. University of Alberta.
- Tsiampousi, A., Zdravković, L., Potts, D. M. 2013. A new Hvorslev surface for critical state type unsaturated and saturated constitutive models. *Computers and Geotechnics*. 48: 156-166.
- Van Genuchten, M. T. 1980. A closed-form equation for predicting the hydraulic conductivity of unsaturated soils. *Soil Science Society of America Journal*. J.44, No. 5, 892 – 898.
- Zdravkovic, L., Potts, D.M., Tsiampousi, A. 2014. Obtaining factors of safety from a finite element analysis of unsaturated soils. In *Unsaturated Soils: research and applications; Proc. 6<sup>th</sup> UNSAT*, Sydney, Australia. Khalili, N., Russell, A.R., Khoshghalb, A. (Eds). CRC Press – Taylor & Francis Group.